THE ASTROPHYSICAL JOURNAL, 449:874–879, 1995 August 20

FURTHER MAPPING OF THE RADIO EMISSION FROM MASSIVE YOUNG STELLAR OBJECTS[1]

MELVIN G. HOARE
Max-Planck-Institut für Astronomie, Königstuhl 17, D-69117 Heidelberg, Germany
AND
SIMON T. GARRINGTON
University of Manchester, Nuffield Radio Astronomy Laboratories, Jodrell Bank, Lower Withington, Cheshire, England, UK SK11 9DL
Received 1994 December 15; accepted 1995 March 7

ABSTRACT

We present high-resolution radio maps at a frequency of 1.6 GHz made with the MERLIN array of the luminous young stellar objects Cep A2 and LkHα 101. The elongation seen previously in Cep A2 appears to extend even farther in our map, supporting a jet interpretation for the morphology of this source. We discuss this and alternative mechanisms in the context of the large-scale outflows in the Cep A region. The 1.6 GHz map of LkHα 101 is more symmetric, although it does show a bright bar of emission at P.A. ≈ 135° plus other extended structures. This map is compared with the previous ones, and overall the ionized wind from this object appears to be far from homogeneous.

Subject headings: ISM: jets and outflows — radio continuum: stars — stars: individual (Cepheus A2, LkHα 101) — stars: pre–main-sequence

1. INTRODUCTION

High-resolution radio continuum observations are beginning to reveal details of the morphology of the ionized mass loss that is a common feature among luminous young stellar objects (YSOs). The winds are expected to recombine about a few hundred AU from the stellar surface (e.g., Höflich & Wehrse 1987) which corresponds to a few tenths of an arcsecond at the typical distances of these objects. The first observations in which this emission was spatially resolved were those of LkHα 101 by Becker & White (1988). This source has a radio spectrum with spectral index α ($S_\nu \propto \nu^\alpha$) of about 0.6 (e.g., Bieging, Cohen, & Schwartz 1984) as expected for thermal emission from a constant velocity outflow (Wright & Barlow 1975). Becker & White (1988) fitted the visibility functions at 1.4, 5, 15, and 22 GHz with an isothermal wind emission and found that the characteristic radius of the emission also scaled with frequency as expected for a constant velocity outflow ($R_C \propto \nu^{-0.6}$). However, they did not discuss possible asymmetries in the wind morphology which could give us important clues to the driving mechanism. This is vital if we are to understand the role, if any, that the ionized wind has in reversing the infall and how it is related to the larger scale bipolar molecular outflow.

Recently, Hoare et al. (1994) mapped LkHα 101 at 5 GHz with a 0.″065 beam using the newly upgraded MERLIN array as well as S106IR, the exciting source of the well-studied bipolar H II region. The latter source has dimensions of 0.″22 × 0.″06 elongated along the equatorial plane. This could possibly be due to either the presence of a remnant disk feeding a radiation-driven wind or rapid rotation of the young star enhancing mass loss in the equatorial direction. The core of LkHα 101, on the other hand, appeared reasonably symmetric, although rather clumpy.

[1] Based on observations made with MERLIN, a national facility operated by the University of Manchester on behalf of PPARC.

Other radio structures have been found on larger scales around luminous YSOs. The most spectacular is the arcminute-long radio jet emerging from either side of the luminous central source of the bipolar nebula GGD 27 and ending in HH objects some 5′ away (Martí, Rodríguez, & Reipurth 1993). In this case, the emission from the jet (where it can be isolated) has a negative spectral index (−0.4 ± 0.1) implying a non-thermal emission mechanism, whilst the core still has a positive index.

A 3″ long radio jet has been seen on one side of S140 IRS 1 by Schwartz (1989), and this also points toward an extended emission region which may be associated with it. A complicating factor here is that the proposed jet is perpendicular to the CO outflow in the region, contrary to expectations. Z CMa is a luminous young binary system where the radio emission is elongated along a position angle within about 20° of the optical jet from this system (Bieging et al. 1984; Skinner, Brown, & Stewart 1993; Poetzel, Mundt, & Ray 1989). The radio counterpart of the very luminous object W3 IRS 5 may also exhibit extended structure (Clausen et al. 1994).

On very small scales Hughes (1988) found that source 2 in Cep A consisted of two components separated by 0.″2 in observations at 15 GHz with 0.″1 resolution, which he interpreted as a young binary system. At slightly lower angular resolution an elongated morphology can be seen with an axial ratio of at least 4:1 (e.g., Hughes 1991; Rodríguez et al. 1994; Hughes, Cohen, & Garrington 1994). With the aid of matching beam observations Rodríguez et al. (1994) interpret this structure as a thermal jet with a spectral index close to 0.6.

Thus, at the moment we appear to be seeing a variety of morphologies and potential mechanisms for the radio emission from luminous YSOs. In order to find out how this fits into a picture for high-mass star formation, we need to map more objects and the same objects over a wider range of frequencies. It is possible that different components dominate at different frequencies, e.g., the thermal central wind at high frequencies

and any nonthermal jet at low frequencies. In this paper we present MERLIN maps of Cep A2 and LkHα 101 at 1.6 GHz with 0".25 resolution.

2. OBSERVATIONS

Observations of LkHα 101 and Cep A were made on 1993 October 4 and 7, respectively, with the full MERLIN array, including the 76 m Lovell telescope at Jodrell and the 32 m telescope at Cambridge, giveing a maximum baseline of 217 km. The observing frequency was 1658 MHz, and the total bandwidth was 15 MHz in each polarization (left-hand circular and right-hand circular). Each source was observed for approximately 8 hr. The initial amplitude and bandpass calibrations were derived from 2134+004 (for LkHα 101) and OQ 208 (for Cep A). The flux densities of these sources were found to be 4.62 and 1.05 Jy, respectively, assuming a flux density of 13.69 Jy for 3C 286. Phase calibrator sources selected from the list of Patnaik et al. (1992) were observed for 2 minutes every 10 minutes (although the Lovell and Wardle telescopes were only driven to the reference source every 30 minutes). The phase calibrator sources were mapped and used to derive amplitude and phase corrections which were interpolated and applied to the target sources. The target source data were weighted according to antenna sensitivity to minimize the noise levels. In the final images the noise levels were 52 μJy for Cep A and 70 μJy for LkHα 101.

3. RESULTS AND DISCUSSION

3.1. *Cepheus A2*

Figure 1 shows the entire region of our 1.6 GHz map of Cep A where significant emission was detected. In this map the Lovell telescope was weighted to give maximum sensitivity, and the resulting resolution is around 0".35. Most of the sources seen previously by Hughes (1988, 1991) are detected, and we adopt his numbering scheme. The principal target Cep A2 is easily detected, and the arc of clumps to the south making up source 3 is also seen. As for the more diffuse sources, only the compact components of sources 1, 4, 6, and 7 are seen. The variable sources 8 and 9 seen by Hughes (1991) are not detected in this map. We list the positions, fluxes, and full widht–half-maxima (FWHMs) of the souces we clearly detect in Table 1. The positions and FWHMs were obtained by fitting a two-dimensional Gaussian component to each source. The total fluxes for sources 3c and 3d are those integrated over a 0".7 and 0".8 box, respectively, centered on the peaks corresponding to the positions given by Hughes (1988). Uncertainties on the fluxes quoted are 1 σ. It can be seen that the 1.6 GHz fluxes of both 3b and 7a appear to have continued to increase compared to those measured in 1982 and 1986 by Hughes (1988).

Source 2 is shown in more detail in Figure 2. Here the Lovell Telescope has been given less weight in order to increase the spatial resolution to about 0".26. This then reveals the elon-

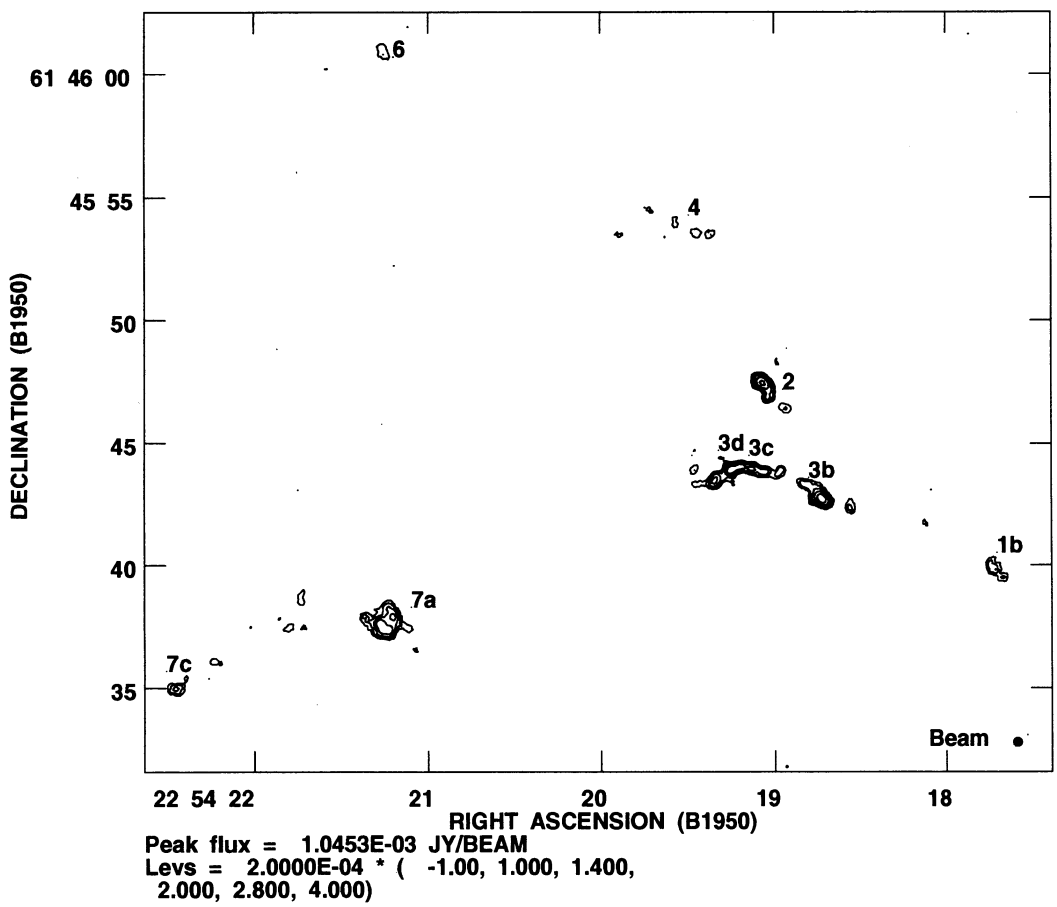

FIG. 1.—1.6 GHz MERLIN map of the Cep A region with a 0".35 circular beam. The contour levels are at −4, 4, 5.6, 8, 11, and 16 times the rms noise level.

TABLE 1

PARAMETERS OF OBSERVED SOURCES IN CEP A2

SOURCE	R.A. (1950) (22^h54^m)	decl. (1950) ($+61°45'$)	FWHM	P.A.	FLUX Peak (mJy)	FLUX Total (mJy)
1b.....	$17^s.706 \pm 0^s.058$	$39''.84 \pm 0''.04$	$1''.11 \pm 0''.06 \times 0''.76 \pm 0''.08$	$51° \pm 12°$	0.4	1.8 ± 0.3
2(ii)	19.066 ± 0.003	47.43 ± 0.01	$0.73 \pm 0.02 \times 0.40 \pm 0.02$	51 ± 3	0.9	2.4 ± 0.1
2(iii).....	19.038 ± 0.005	46.84 ± 0.01	0.45 ± 0.03	...	0.5	0.7 ± 0.1
3b.....	18.732 ± 0.005	42.76 ± 0.02	$0.87 \pm 0.04 \times 0.53 \pm 0.02$	45 ± 5	1.0	4.2 ± 0.2
3c.....	19.070 ± 0.006	43.83 ± 0.01	$0.81 \pm 0.02 \times 0.41 \pm 0.07$	82 ± 4	0.5	0.9 ± 0.1
3d.....	19.248 ± 0.008	43.93 ± 0.02	$0.87 \pm 0.04 \times 0.50 \pm 0.09$	114 ± 8	0.7	1.7 ± 0.1
7a.....	21.248 ± 0.007	37.66 ± 0.02	$1.32 \pm 0.04 \times 1.11 \pm 0.04$	99 ± 11	0.8	7.6 ± 0.3
7c.....	22.439 ± 0.011	34.98 ± 0.03	$0.86 \pm 0.05 \times 0.62 \pm 0.08$	93 ± 16	0.4	1.6 ± 0.2

gated structure of the main component (2[ii]) as seen in previous observations (Hughes 1991; Rodríguez et al. 1994; Hughes et al. 1994). A new component which we label 2(iii) is revealed to the south of the main component. A hint of this component can be seen as an extension in the contours southward in the 0".3 resolution 5 GHz maps of Hughes (1991). The FWHMs given in Table 1 for sources 2(ii) and 2(iii) were determined from the map in Figure 2 by fitting two Gaussians simultaneously, one representing the elongated source and one for 2(iii). There is another patch of emission about 1".4 to the SW of the main component which is more significant in the lower resolution map in Figure 1. Integrated over the whole area of source 2, the total flux is about 3.3 mJy, which is in good agreement with the 1.49 GHz flux measured by Rodríguez et al. (1994) in 1991. This value is much higher than those observed by Hughes (1988) in 1982 and 1986, and it would appear that the flux is increasing with time.

The mean positions for components 2(i) and 2(ii) from Hughes (1988) and Hughes et al. (1994) which have uncertainties of 0".03 are plotted as crosses in Figure 2. It can be seen that the peak of the main component coincides with component 2(ii). However, in our data 2(i) does not appear to be a separate component but merely the bright beginning of the extension to the SW. The position angle for 2(ii) in Table 1 agrees to within the errors with the 48° derived by Rodríguez et al. (1994) from 0".2 resolution 8.4 GHz data. If we fit only the bright core of our 1.6 GHz map, we obtain a position angle of $45° \pm 3°$. A line at this position angle is seen to go through the patches of emission to the SW of 2(ii) in Figure 2, which are the peaks of the more extended patch seen in Figure 1. Although there appears to be a gap between this emission and the main component, the alignment is somewhat suggestive. If this emission is associated with 2(ii), then it is the farthest extension seen in any radio maps of this object so far. Such an elongation would suggest that the radio morphology of Cep A2 may be explained as an ionized jet. This interpretation is also favored by Rodríguez et al. (1994) from the morphology of their 8.4 GHz map. At that frequency the source looks more two-sided, whereas our 1.6 GHz map has a more one-sided appearance, rather like S140 IRS 1 and W3 IRS 5. In fact, above 5 GHz all the previous high-resolution maps show a more equal brightness of the two lobes, whereas at 5 GHz and below the SW lobe is always the more dominant.

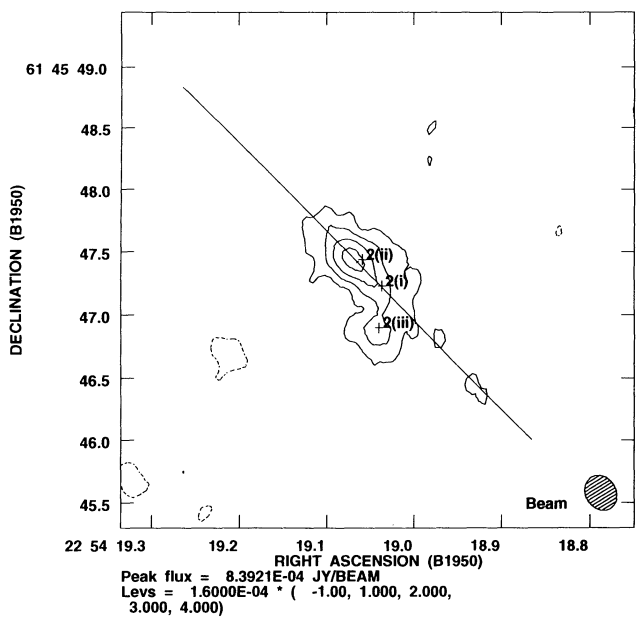

FIG. 2.—1.6 GHz MERLIN map of Cep A2 with a 0".29 × 0".24 beam at P.A. = 31°.6. Contour levels are at −3, 3, 6, 9, 12, and 15 times the rms noise. The solid line is at P.A. = 45°.

If the source is a jet, then the orientation is somewhat surprising. The outflow activity in the region which is usually thought to originate from Cep A2 has an E-W axis as revealed by optical HH objects and near-IR shocked molecular hydrogen emission (Corcoran, Ray, & Mundt 1993). The OH masers associated with Cep A2 have an E-W segregation in their radial velocities (Cohen, Rowland, & Blair 1984), and observations of high-velocity CO emission show that the brightest emission is also aligned E-W (P.A. ≈ 100°) (Bally & Lane 1991; Moriarty-Schieven, Snell, & Hughes 1991; Torrelles et al. 1993). There is evidence for another bipolar flow at a position angle of about 25°–30°, although this flow does not appear to be centered on Cep A2. None of these flows are at a position angle of 45°.

The bright IR reflection nebula in Cep A does lie to the NE of source 2, which from the polarization vectors is likely to be its illuminating source (Lenzen, Hodapp, & Solf 1984; Hodapp 1990). The general IR appearance gives the impression of a dark lane running SE-NW through the position of Cep A2. If the source really has a bipolar structure as seen in many YSOs, then presumably we only see the NE lobe of the reflection nebula, since the SW lobe is tilted away from us and is either obscured by a flattened distribution of circumstellar material or is buried deeper in the molecular cloud if the source happens to be on the near side of the cloud. The latter could perhaps explain why the SW lobe of Cep A2 is dominant at lower

frequencies, because the jet is ploughing into denser material on this side which gives rise to HH-like activity, which as has been seen in the case of HH 80 can be characterized by a more negative spectral index. A recent *K*-band image of a wide field around Cep A also reveals a cone of emission ending in a bright arc about 2′ to the SW of Cep A2 with its apex close to Cep A2 (M. McCaughrean 1994, private communication). This emission does not appear in a subsequent continuum-subtracted narrowband image in the molecular hydrogen 1–0 *S*(1) line and is therefore not a molecular outflow, but a connection with the SW lobe of Cep A2 is still a possibility.

An alternative explanation for the elongated radio morphology of Cep A2 is that as in the case of S106IR (Hoare et al. 1994) the elongation of the source is in the equatorial plane and is somehow associated with a disk. The submillimeter continuum emission from the region, which is a good tracer of overall column density, also has a P.A. $\approx 40°$ (Moriarty-Schieven et al. 1991). If any small-scale disk structure had the same orientation as the larger scale molecular cloud, then this would be consistent with a disk-influenced interpretation for the radio morphology for Cep A2. However, if there is a disk at P.A. $\approx 45°$, then any associated bipolar outflow should have a P.A. $\approx 135°$, which is also not consistent with any of the observed outflows.

Hughes (1988), in light of his 15 GHz map of Cep A2 which showed a double radio source, proposed that it was a binary system. However, subsequent high-resolution radio maps do not always show this structure (Hughes 1991), and in the very high resolution 5 GHz MERLIN map by Hughes et al. (1994) source 2(i) is completely resolved into a series of clumps, while 2(ii) remains unresolved. We prefer the interpretation that source 2(i) is just the beginning of the elongation SW of the dominant 2(ii) component which is the driving source, but further observations are needed to confirm this picture.

The nature of the newly resolved source 2(iii) is not clear. It seems to have a fairly negative spectral index since it appears in the 0.″3 resolution 5 GHz maps of Hughes (1991) at about the 0.2 mJy beam^{-1} level and not at all in the 15 GHz maps. In the jet scenario it could be another patch of HH-like emission like that farther to the SW although it is some way off the axis. High spatial resolution thermal-IR imaging is required to determine the spatial distribution of material close to Cep A2 which may then enable us to distinguish between the various scenarios for the radio morphology. This source is so deeply embedded that it does not show up at the *K* or *L* IR bands (Lenzen, Hodapp, & Solf 1984; Hodapp 1990).

3.2. *LkHα 101*

A MERLIN 1.6 GHz map including the Lovell Telescope of LkHα 101 at a resolution of 0.″23 is presented in Figure 3. The peak flux in our map corresponds to a brightness temperature of about 14,000 K. This is similar to the peak brightness temperature found from our 5 GHz observations but higher than the electron temperature of around 7500 K determined by Becker & White (1988) from modeling the 1.4 GHz visibility function. The integrated flux from our 1.6 GHz map is 10.0 ± 0.5 mJy, in good agreement with the 10.8 ± 0.6 mJy measured by Becker & White (1988) at 0.″8 resolution with the VLA. Assuming a distance of 0.8 kpc and fully ionized gas at a temperature of 10^4 K, we find that our 1.6 GHz flux implies a mass-loss rate of $2.6 \times 10^{-8} v_\infty$ (km s^{-1}) $M_\odot$ yr^{-1} (Wright & Barlow 1975), which is in reasonable agreement with that derived by Cohen, Bieging, & Schwartz (1982). The terminal

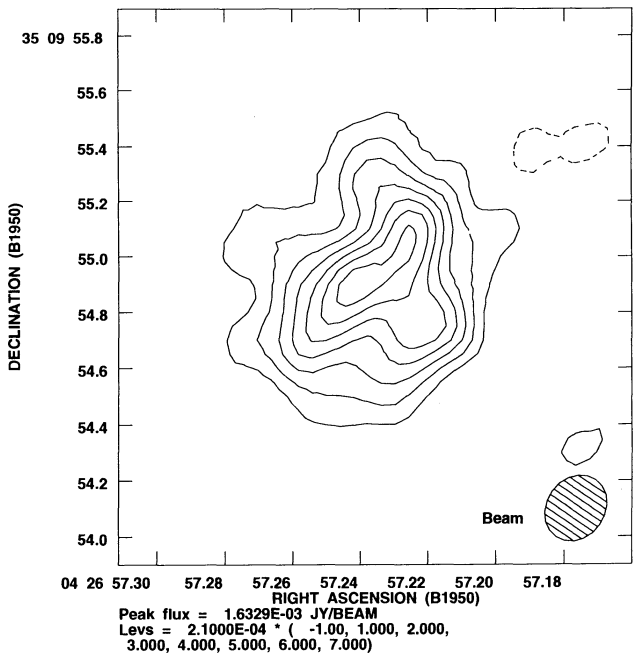

FIG. 3.—1.6 GHz MERLIN map of LkHα 101. The beam size is 0.″25 × 0.″21 at P.A. = −34°. Contour levels are at −3, 3, 6, 9, 12, 15, 18, and 21 times the rms noise.

velocity is not well known for LkHα 101. Hamann & Persson (1989) have shown that the very high velocity wings on the Hα line could be due to electron scattering but that there is still excess emission up to velocities of about 350 km s^{-1}. This corresponds to the broad weak wing on the Brγ line (Simon & Cassar 1984), although there is a need for high signal-to-noise ratio, high-resolution spectra of the IR lines to constrain the terminal velocity more accurately.

As in the 5 GHz MERLIN map (Hoare et al. 1994), the overall structure of LkHα 101 is reasonably symmetric. A fit to the whole source gives a deconvolved size of 0.″63 × 0.″48 (P.A. = 151° ± 6°). The mean size of 0.″55 is therefore close to the 5 GHz size (0.″31) scaled by $\nu^{-0.6}$ as expected for a stellar wind (Wright & Barlow 1975). Using the mass-loss rate derived above, we find that the characteristic radius of the emitting region is 2.8×10^{15} cm or a diameter of 0.″45 at 0.8 kpc, in reasonable agreement with the observed size.

The dominant asymmetrical structure is a bright bar of emission in the core running from SE to NW. When a Gaussian fit is applied to an area restricted to the bright core, we obtain a size of 1.″0 × 0.″5 at position angle 134° ± 11°. We have also made á uniformly weighted map excluding the Lovell telescope, which has a resolution of 0.″13, although the noise level is considerably higher. The bar of emission then breaks up into two spots on either side of the peak, although they are not exactly aligned and would seem to indicate that it is not a continuous linear feature. However, one has to be careful not to overinterpret features in this map since the source is very overresolved at this resolution.

Fainter extensions can also be seen to the SW, N, and ENE of the peak in Figure 3. Bieging et al. (1984) also mapped LkHα 101 at 5 and 15 GHz with 0.″6 and 0.″3 beams, respectively. Their maps show some resolved structure as well, notably extensions to the ENE and SW which may correspond to similar features seen here, although they question the reality

of their ENE extension. In order to check the credibility of the extensions we mapped a simulated ring with a similar size and peak flux as LkHα 101 with the same array as used in the observations. The simulated map, which has the same noise level as the observed one, only showed significant deviations from circular at 15% of the peak flux level. The structure in Figure 3 is at a much higher level than this and is therefore reliable.

At first glance, the 1.6 GHz map bears little resemblance to the clumpy, more symmetric appearance of the 0".065 resolution 5 GHz MERLIN map by Hoare et al. (1994). However, in Figure 4 we show the 5 GHz data with a 3 Mλ taper applied and CLEANed with a circular beam of FWHM = 0".15. This beam size is close to the resolution of the 1.6 GHz map scaled down by $\nu^{-0.6}$. There is possibly some correspondence now between the lower intensity extended features at the two different frequencies. The bright bar of emission at P.A. = 134° ± 11° does not appear as a strong feature in the 5 GHz map. This may be due to different components dominating at the two frequencies. Overall, LkHα 101 appears to have a clumpy, slightly asymmetric wind, although the average density distribution has the r^{-2} law expected for a constant velocity outflow (Becker & White 1988).

Unfortunately, there is little evidence for outflows on a larger scale in this object with which to try and relate the modest radio asymmetry. There is CO emission from a few ambient molecular clouds, but no ordered velocity field such as a bipolar flow has been seen (Redman et al. 1986; Barsony et al. 1990). The VLA map of the H II region surrounding LkHα 101 from Becker & White (1988) shows two clumpy arcs of emission extending up to 20" away from the star in a pattern reminiscent of the spiral arms of a galaxy. It is unclear if or how this structure is related to the high-resolution radio morphology. Optical photographs show a dark lane running from NE to SW on the edge of which the star itself is located, although Redman et al. (1986) believe that this cloud is a foreground feature and not directly associated with LkHα 101.

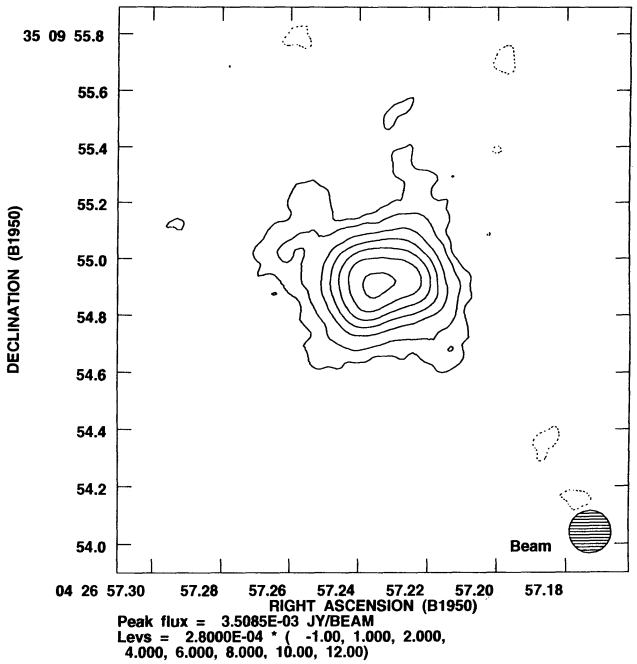

FIG. 4.—5 GHz MERLIN map of LkHα 101 with a 3 Mλ taper applied and CLEANed with a 0".15 circular beam. Contour levels are at −3, 3, 6, 12, 18, 24, 30, and 36 times the rms noise.

4. CONCLUDING REMARKS

These observations show that the morphology of the radio emission from luminous YSOs is far from symmetric, varies greatly from object to object, and also perhaps varies with frequency for individual objects. Of course, the definition of a luminous YSO itself is far from homogeneous, with one of our targets being a deeply embedded IR source powering maser activity and probably outflows, while the other is a visible star with an extended H II region. LkHα 101 is, like the exciting source of S106, presumably more evolved than Cep A2 and other deeply embedded YSOs. Before significant conclusions can be drawn on the various morphologies and possible driving mechanisms, a wider sample of objects needs to be mapped which spans the range of masses and evolutionary stages of young OB stars. This will be difficult since most of the remaining known massive YSOs are less luminous than Cep A2 or S106IR at radio wavelengths which are already near the limit of current capabilities of interferometers with sufficiently long baselines to resolve the objects.

An additional way that we may be able to extend the sample further is to obtain diffraction-limited near-IR images (≈0".1 resolution) which could reveal structures related to the various radio morphologies. It is also important to relate the radio results to the other principal means of studying these winds: that of high spectral resolution IR line profiles (e.g., Drew et al. 1993; Bunn, Hoare, & Drew 1995). To our knowledge none of the sources with a jet morphology (Cep A2, GGD 27–Ill, S140 IRS 1 and W3 IRS 5) have been observed in this way.

MERLIN is a UK national facility operated by the University of Manchester on behalf of PPARC. We thank the staff at NRAL for their assistance in making the observations with MERLIN. Useful discussions on the interpretation of the data were held with Janet Drew (Oxford) and Mark McCaughrean (MPIA), who made available new IR images. We are grateful to the anonymous referee whose recommendations improved the completeness of the paper. M. G. H. acknowledges the financial support of the MPG.

REFERENCES

Bally, J., & Lane, A. P. 1991, in Astrophysics with Infrared Arrays, ed. R. Elston (ASP Conf. Ser., 14), 273
Barsony, M., Scoville, N. Z., Schombert, J. M., & Claussen, M. J. 1990, ApJ, 362, 674
Becker, R. H., & White, R. L. 1988, ApJ, 324, 893
Bieging, J. H., Cohen, M., & Schwartz, P. R. 1984, ApJ, 282, 699
Bunn, J. C., Hoare, M. G., & Drew, J. E. 1995, MNRAS, 272, 346
Clausen, M. J., Gaume, R. A., Johnston, K. J., & Wilson, T. L. 1994, ApJ, 424, L41
Cohen, M., Bieging, J. H., & Schwartz, P. R. 1982, ApJ, 253, 707
Cohen, R. J., Rowland, P. R., & Blair, M. M. 1984, MNRAS, 210, 425
Corcoran, D., Ray, T. P., & Mundt, R. 1993, A&A, 279, 206
Drew, J. E., Bunn, J. C., & Hoare, M. G. 1993, MNRAS, 265, 12
Hamann, F., & Persson, S. E. 1989, ApJS, 71, 931
Hoare, M. G., Drew, J. E., Muxlow, T. B., & Davis, R. J. 1994, ApJ, 421, L51
Hodapp, K.-W. 1990, ApJ, 352, 184
Höflich, P., & Wehrse, R. 1987, A&A, 185, 107
Hughes, V. A. 1988, ApJ, 333, 788
———. 1991, ApJ, 383, 280
Hughes, V. A., Cohen, R. J., & Garrington, S. 1994, MNRAS, 272, 469

Lenzen, R., Hodapp, K.-W., & Solf, J. 1984, A&A, 137, 202
Martí, J., Rodríguez, L. F., & Reipurth, B. 1993, ApJ, 416, 208
Moriarty-Schieven, G. H., Snell, R. L., & Hughes, V. A. 1991, ApJ, 374, 169
Patnaik, A. R., Browne, I. W. A., Wilkinson, P. N., & Wrobel, J. M. 1992, MNRAS, 254, 655
Poetzel, R., Mundt, R., & Ray, T. P. 1989, A&A, 224, L13
Redman, R. O., Kuiper, T. B. H., Lorre, J. J., & Gunn, J. E. 1986, ApJ, 303, 300
Rodríguez, L. F., Garay, G., Curiel, S., Ramírez, S., Torrelles, J. M., Gómez, Y., & Velázquez, A. 1994, ApJ, 430, L65
Schwartz, P. R. 1989, ApJ, 338, L25
Skinner, S. L., Brown, A., & Stewart, R. T. 1993, ApJ, 87, 217
Simon, M., & Cassar, L. 1984, ApJ, 283, 179
Torrelles, J. M., Verdes-Montenegro, L., Ho, P. T. P., Rodríguez, L. F., & Cantó, J. 1993, ApJ, 410, 202
Wright, A. E., & Barlow, M. J. 1975, MNRAS, 170, 41